ORBIT ROENTGENOLOGY

EDITED BY
PETER H. ARGER

Orbit Roentgenology

Edited by

Peter H. Arger, M.D.

Associate Professor of Radiology
Hospital of the University of Pennsylvania
Philadelphia, Pennsylvania

A WILEY MEDICAL PUBLICATION

JOHN WILEY & SONS

New York/Chichester/Brisbane/Toronto

Library of Congress Cataloging in Publication Data:

Main entry under title:

Orbit roentgenology.

(Wiley series in diagnostic and therapeutic radiology)
(A Wiley medical publication)
Includes bibliographies and index.
1. Eye-sockets—Radiography. I. Arger, Peter H.
[DNLM: 1. Orbit—Radiography. WH141 064]
RE79.R307 617.7'8'07572 77-23447
ISBN 0-471-03310-3

Printed in the United States of America

10 9 8 7 6 5 4 3 2

Orbit Roentgenology

Wiley Series in Diagnostic and Therapeutic Radiology

Luther W. Brady, M.D., Editor

Professor and Chairman, Department of Therapeutic Radiology and Nuclear Medicine, Hahnemann Medical College and Hospital, Philadelphia, Pennsylvania

TUMORS OF THE NERVOUS SYSTEM

Edited by H. Gunter Seydel, M.D., M.S.

CANCER OF THE LUNG

By H. Gunter Seydel, M.D., M.S.
Arnold Chait, M.D.
John T. Gmelich, M.D.

CLINICAL APPLICATIONS OF THE ELECTRON BEAM

Edited by Norah duV. Tapley, M.D.

NUCLEAR OPHTHALMOLOGY

Edited by Millard Croll, M.D.
Luther W. Brady, M.D.
Paul Carmichael, M.D.
Robert J. Wallner, D.O.

HIGH-ENERGY PHOTONS AND ELECTRONS:
Clinical Applications in Cancer Management

Edited by Simon Kramer, M.D.
Nagalingam Suntharalingam, Ph.D.
George F. Zinninger, M.D.

TRENDS IN CHILDHOOD CANCER

Edited by Milton H. Donaldson, M.D.
H. Gunter Seydel, M.D., M.S.

ABDOMINAL GRAY SCALE ULTRASONOGRAPHY

Edited by Barry B. Goldberg, M.D.

ORBIT ROENTGENOLOGY

Edited by Peter H. Arger, M.D.

To Afento H. Arger,
a unique woman who made anything possible

Contributors

William E. Allen III, M.D., Associate Professor of Diagnostic Radiology, Yale University School of Medicine, New Haven, Connecticut

Melvin G. Alper, M.D., Clinical Professor of Ophthalmology and Neurosurgery, George Washington University Medical Center, Washington, D.C.

Peter H. Arger, M.D., Associate Professor of Radiology, Hospital of the University of Pennsylvania, Philadelphia, Pennsylvania

Larissa T. Bilaniuk, M.D., Assistant Professor of Radiology, Hospital of the University of Pennsylvania, Philadelphia, Pennsylvania

Paul L. Carmichael, M.D., Clinical Associate Professor of Ophthalmology, Thomas Jefferson University School of Medicine; Visiting Associate Professor of Nuclear Medicine, Hahnemann Medical College Hospital, Philadelphia, Pennsylvania; Associate Surgeon, Retina Service, Wills Eye Hospital, Philadelphia, Pennsylvania

Claude Clay, M.D., A.I.H.P., Chef de Clinique, Hôtel Dieu, Paris, France

David O. Davis, M.D., Professor and Associate Chairman, Department of Radiology, George Washington University Medical Center, Washington, D.C.

Joseph C. Flanagan, M.D., Associate Surgeon, Oculoplastic Service, Wills Eye Hospital, Philadelphia, Pennsylvania; Associate Professor of Ophthalmology, Thomas Jefferson University School of Medicine, Lankenau Hospital, Philadelphia, Pennsylvania

Pierre Lasjaunias, M.D., Fondation Ophtalmologique Rothschild, Paris, France

Jerrold Mink, M.D., UCLA Center for the Health Sciences, Los Angeles, California

Jacques Moret, M.D., Service de Radiologie, Fondation Ophtalmologique Rothschild, Paris, France

Karl Ossoinig, M.D., Professor of Ophthalmology, Department of Ophthalmology, University of Iowa, Iowa City, Iowa

Stephen L. G. Rothman, M.D., Associate Professor of Diagnostic Radiology, Yale University School of Medicine, New Haven, Connecticut

Jacqueline Vignaud, M.D., Chef de Service de Radiologie, Fondation Ophtalmologique Rothschild, Paris, France

Robert A. Zimmerman, M.D., Assistant Professor of Radiology, Hospital of the University of Pennsylvania, Philadelphia, Pennsylvania

Series Preface

The past five years have produced an explosion in the knowledge, techniques, and clinical application of radiology in all of its specialities. New techniques in diagnostic radiology have contributed to a quality of medical care for the patient unparalleled in the United States. Among these techniques are the development and applications in ultrasound, the development and implementation of computed tomography, and many exploratory studies using holographic techniques. The advances in nuclear medicine have allowed for a wider diversity of application of these techniques in clinical medicine and have involved not only major new developments in instrumentation, but also development of newer radiopharmaceuticals.

Advances in radiation therapy have significantly improved the cure rates for cancer. Radiation techniques in the treatment of cancer are now utilized in more than 50% of the patients with the established diagnosis of cancer.

It is the purpose of this series of monographs to bring together the various aspects of radiology and all its specialties so that the physician by continuance of his education and rigid self-discipline may maintain high standards of professional knowledge.

LUTHER W. BRADY, M.D.

Preface

The aim of this book is to provide physicians with the information necessary to provide the best possible care for patients with orbit problems. Although the orbit comprises only a small area of the body, it is involved in many varied disease processes. The physicians who care for patients with orbit problems need an in-depth knowledge of orbit anatomy and the diagnostic modalities available to analyse such problems. With this knowledge, they can obtain the diagnostic procedure that will give the most information about the problem.

As the editor, I felt that to develop thorough coverage of a diagnostic area most effectively required the participation and contributions of a number of specialists. I was most fortunate in obtaining the cooperation of an enthusiastic and distinguished group of contributors. This book is as much theirs as it is mine, and I am profoundly grateful to them.

I must also acknowledge the dedicated efforts of Mrs. Barbara Gallagher, for her help with the voluminous contributor correspondence and manuscript typing necessary for completion of the book, and Dr. John Bonavita, whose French translation made it possible for me to include the marvelous work of Dr. Jacqueline Vignaud and her colleagues.

PETER H. ARGER, M.D.

Roentgen Anatomy of the Orbit

Jacqueline Vignaud, M.D.
Chef de Service de Radiologie
Fondation Ophtalmologique Rothschild
Paris, France

Claude Clay, M.D., A.I.H.P.
Chef de Clinique
Hôtel Dieu
Paris, France

Jerrold Mink, M.D.
UCLA Center for the Health Sciences
Los Angeles, California

The bony orbits are the two recesses situated between the anterior cranial fossa above and the maxillary sinuses below. They are bounded medially by the ethmoid sinuses, which separate them from the nasal cavities. Classically, the orbits are described as quadrangular pyramids whose axes are directed posteromedially from the anteriorly situated base. If these axes were extended posteriorly, they would cross each other at an angle of 40 to 45°. The axis of the lateral wall of the orbit would nearly define the long axis of the petrous pyramid of the opposite side.

The orbits have a depth that varies, as measured along their axes, of 42 to 50 mm; the base measures (mean) 40 mm in width and 35 mm in height. The distance between the orbits, as defined by Broca, is 25 mm. The relationship between the height and width, given by height/width × 100, yields an index that varies among the species of man. Orientals, whose index is >89, are defined as "megasènes"; Caucasians, called "mesosènes," have an index between 83 and 89; blacks, with an index of <83, are termed "microsènes."

The bony orbit houses the eyeball and its appendages, including the ocular muscles, their nerves, and their common tendon sheath that insures both the stability and mobility of the globe; the lacrimal and palpebral glands, whose secretions moisten the cornea and thereby protect it; the nasolacrimal apparatus; an arterial supply fed by the internal carotid artery and the external carotid; a largely anastomosed venous system, including the superior and inferior ophthalmic veins; oculomotor and sensitive nerves; and, finally, the orbital fat that fills the remainder of the orbit and furthermore serves as a shock absorber.

Serial frontal anatomical sections allow a better understanding of the relationship between the different components of the orbit (Figs. 1*a* to *f*).

THE BONY ORBIT

Our approach will integrate the gross anatomy with the radiologic finding, including standard (Figs. 2 to 6) and tomographic views (Figs. 7 to 10).

Seven separate bones (Figs. 11 to 13) comprises the orbit, which will be described as having four walls, four angles, and a base.

The Superior Orbital Wall (Roof of the Orbit)

The horizontal lamina of the frontal bone and the orbital surface of the lesser sphenoid wing, forming the triangular orbital roof, meet at the frontosphenoid suture, which is situated at the junction of the anterior two thirds and posterior one third of the roof (Figs. 11, 12). One can identify the trochlea fossa, in which the fibrous loop for the tendon of the superior oblique muscle is inserted (the loop itself may insert on a small protuberance, the trochlear spine) (Fig. 13).

The roof of the orbit is also the floor of the anterior cranial fossa. This is of variable thickness because of the presence of the convolutional markings of the inferior surface of the frontal lobe (Fig. 12), which create areas of relative radiolucency. Thus, the standard radiographs (Figs. 2 to 6), including the Caldwell projection (Fig. 2) (the central ray is inclined −25° to the orbitomeatal line, OM), and the Waters projection (Fig. 4) (the central ray is inclined −50° to OM) do not yield optimal visualization of the roof. Tomograms often prove helpful in evaluating the integrity of the bone. It should also be mentioned that the floor of the frontal sinus is related to the orbital roof (Figs. 8*a* to 10*b*), especially when the inferior recess of the sinus is well developed. This fact may assume some importance in cases of sinus tumors or mucoceles.

When performing frontal-plane tomography, several projections may be used. For evaluations of the orbital roof, we prefer a view in which the orbitomeatal line is perpendicular to the film (Fig. 8). If the head is inclined slightly (−30° with respect to the OM line) (Fig. 7), the impressions of the frontal lobe distort the image of the roof (Fig. 7*c*, *d*). Lateral tomograms are both complementary and necessary for definitive evaluation.

The Medial Wall of the Orbit

The medial wall is parallel to the sagittal plane of the skull. It is quadrilateral in shape and is composed of (from back to front) the body of the sphenoid, the orbital plate of the ethmoid, the lacrimal bone, and the frontal process of the maxilla (Figs. 11 to 13). The lacrimal groove (formed by the lacrimal crests of the lacrimal bone posteriorly, the maxillary bone anteriorly, and the lacrimomaxillary suture medial) is located anteriorly on this wall. The posterior lip of this groove ends in a protuberance known as the hamulus lacrimalis, part of the orifice of the nasolacrimal canal into which the groove opens.

The lacrimal bone itself, because of its position and thinness, is quite difficult to visualize on radiographs. However, tomography in the frontal (perpendicular or −30° with respect to the OM line) (Fig. 7*a*) and lateral position (Fig. 10*b*) will demonstrate the nasolacrimal canal. This canal is bounded laterally by the pyramidal process of the maxilla and is closed medially by the inferior turbinate. It descends from the orbit to open into the nasal cavity, just below the inferior turbinate.

This is an appropriate time to mention dacryocystography (radio-opaque visualization of the nasolacrimal apparatus). After coursing over the globe, the tears enter the nasolacrimal apparatus (Figs. 14, 15) through the puncta, two small

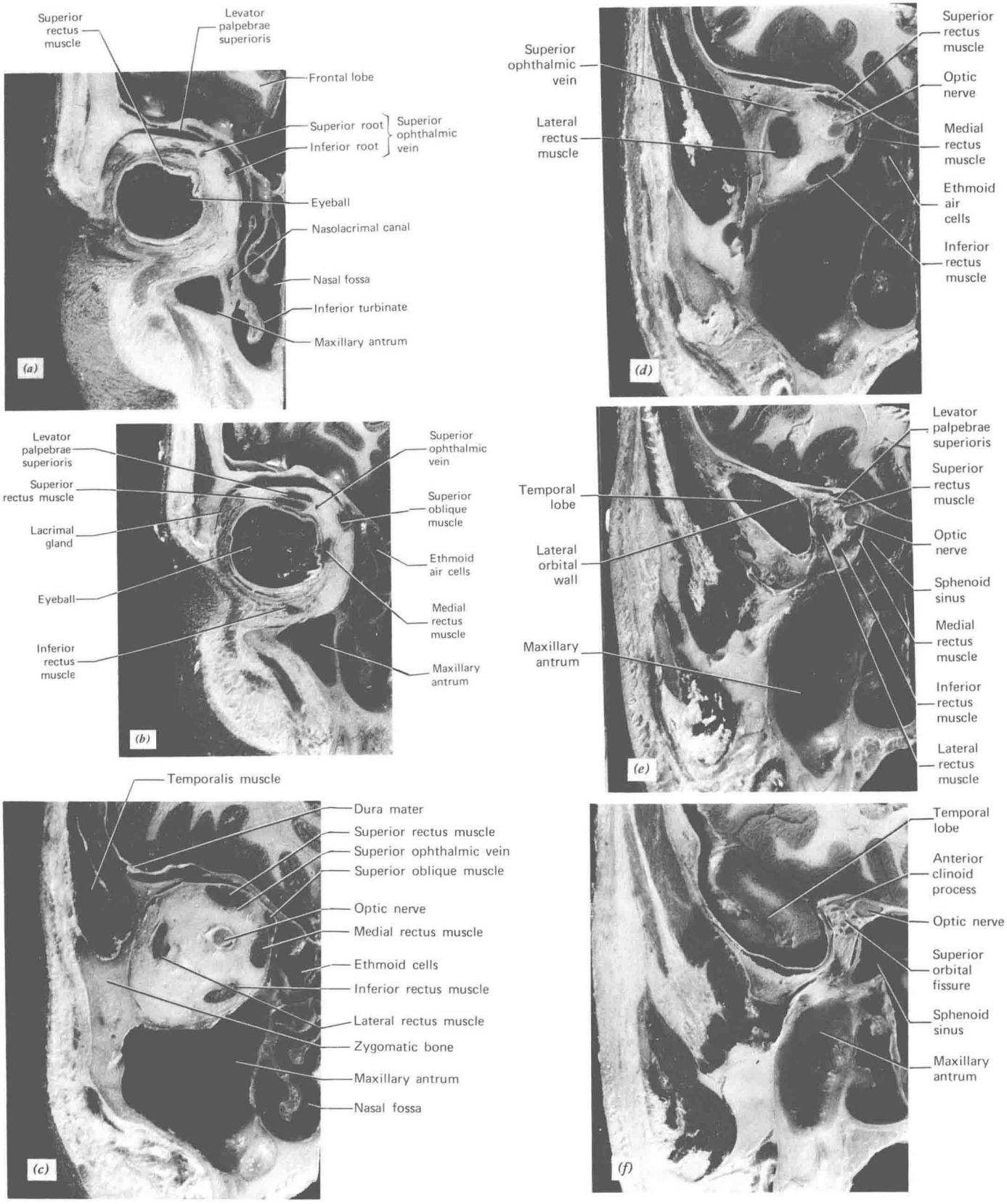

Fig. 1. Serial frontal anatomical sections, from front to back. Courtesy of R. Paleirae.

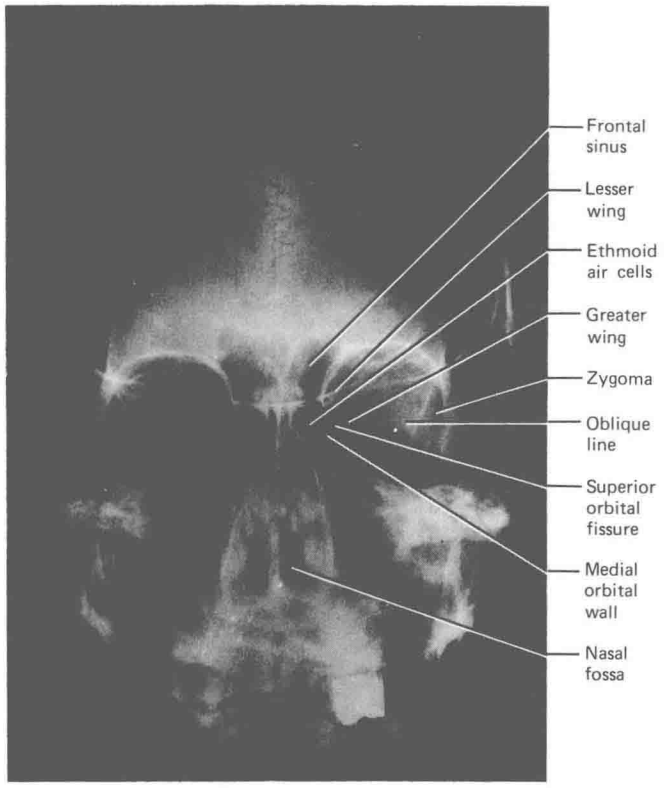

Fig. 2. PA view. OM = −25°.

orifices, one at either eyelid, each of which opens into a canaliculus. The latter is a small canal running medially in the edge of each eyelid to join its fellow at the medial canthus of the eye. At this point, there is a slight dilatation in the common channel known as the sinus of Maier. This, in turn, opens into the nasolacrimal sac, which is housed in the lacrimal groove. The sac then tapers as it descends in the nasolacrimal canal to terminate under the inferior turbinate. The walls of the duct are not perfectly smooth. There are zones of relative narrowing and areas of dilatation. Many authors have described these areas of tapering as "valvulae" and have ascribed their names to them. It is probably best to consider these valvulae as plications of the mucosa and probably inconstant, normal variants.

While performing dacryocystography, we make tomographic sections of the nasolacrimal apparatus. This yields three important pieces of information.

1. One can accurately evaluate the bony canal.
2. One can assess the thickness of the nasal mucosa over the inferior turbinate (this may be a cause of tearing).
3. One can determine the proximity of the anterior ethmoid air cells to the canal (this is important in planning any operative intervention) (Fig. 15).

The medial orbital wall is the thinnest. It is seen on the routine PA views (−25° or −35° with respect to the OM line) (Figs. 2, 3). However, on the Waters projection (−50°) (Fig. 4), only the most anterior portion of the wall can be seen. Basal (Fig. 9*a*, *b*, *c*) and AP tomograms (Figs. 7*b*, *c*, *d*) and 8*a*, *b*, *c*, *d*) provide more complete evaluation. In these projections, the intimate relation of the wall to the ethmoid air cells and the anterior part of sphenoid sinus is best seen. The continuity of this wall may be jeopardized in cases of sinus or orbital pathology, including trauma. The extent of such a lesion must be accurately known in order to decide on proper therapy.

The Superior Internal Angle. The superior internal angle is traversed by the frontolacrimal suture and the ethmoidofrontal suture. The ethmoidal canals open into the latter. The anterior canal is the larger of the two. It transmits:

1. The anterior ethmoidal artery, a branch of the ophthalmic artery.
2. The internal nasal nerve, derived from the nasal branch of the ophthalmic nerve of Willis. This nerve leaves the orbit through the anterior canal, reaches the cribriform plate, passes down the ethmoid groove and, finally, enters the nasal fossa through the anterior ethmoid foramen. This exquisitely sensitive nerve is the sensory channel for the cornea, nasal septum, lateral walls of the nasal fossa, and the skin of the alae of the nose.
3. The anterior ethmoidal vein, which is usually quite small.

The posterior ethmoid canal is quite small. It is approximately 3.5 cm from the orbital rim (1.5 cm behind the anterior canal). It transmits:

1. The posterior ethmoidal artery, also a branch of the ophthalmic artery.
2. The sphenoethmoidal nerve of Luschka, a branch of the nasal nerve that innervates the wall of the sphenoid sinus and the posterior ethmoid cells.
3. The small posterior ethmoidal vein.

These two channels, although seen in the dried specimen, are not seen in conventional or tomographic X-ray examinations because of their size and the thinness of their walls.

The Inferior Orbital Wall (Floor of the Orbit)

The floor of the orbit is the roof of the maxillary sinus. This, coupled with the fact that the floor is quite thin,

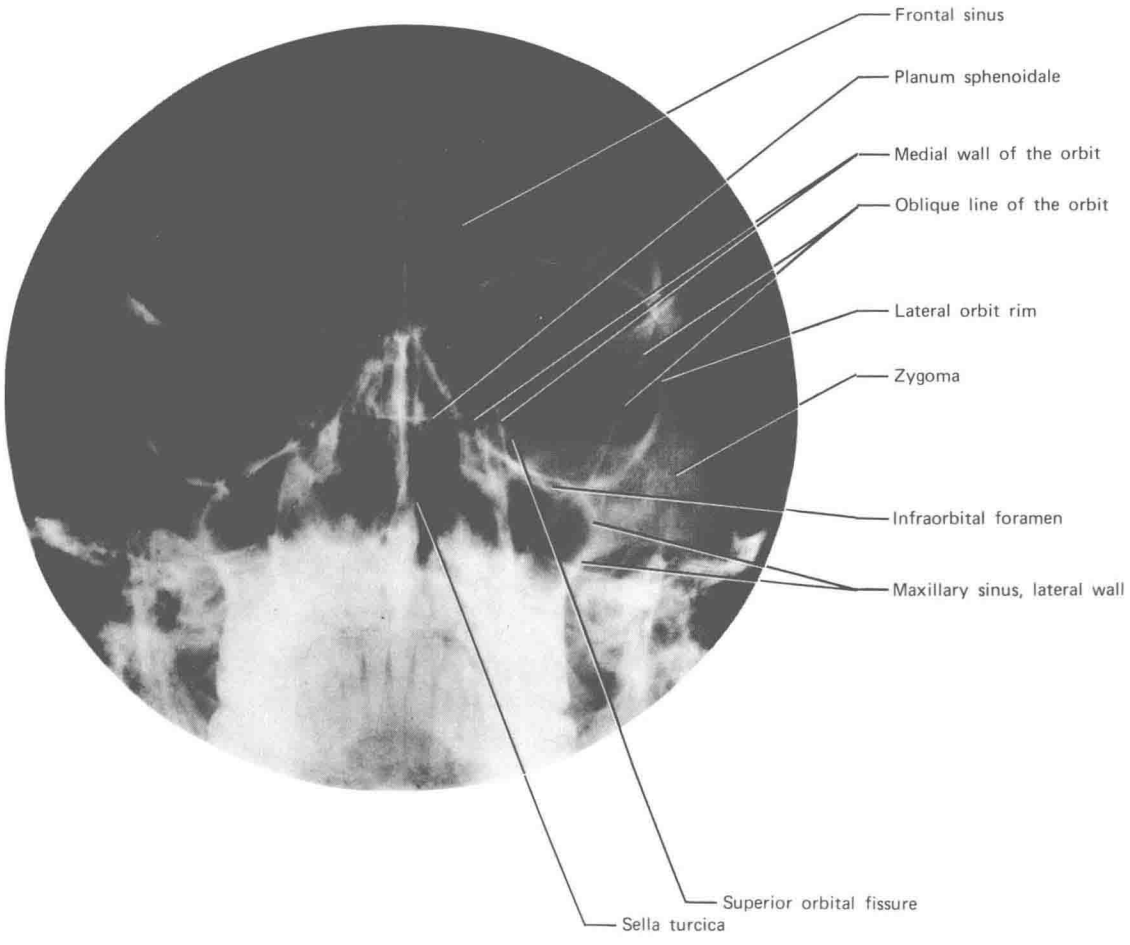

Fig. 3. PA view. OM = −35°.

assumes importance in cases of trauma in which blow-out fractures are a consideration.

The orbital surface of the pyramid process of the maxillary bone medially and the orbital surface of the zygoma laterally comprise the orbital floor. There is a small contribution posteriorly from the palatine bone (Fig. 11). The floor is bounded laterally by the infraorbital fissure and medially by the suture that unites the palatine, ethmoid, and lacrimal bones to the orbital surface of the maxilla.

The floor of the orbit bears a groove (Fig. 11) running posteroanteriorly. After a 2 cm path, the groove is completed superiorly to extend as a canal (Figs. 3, 4, 7*b*). The canal opens as the infraorbital foramen just below the infraorbital rim (Fig. 13), transmitting the infraorbital nerve (a branch of V2), the infraorbital artery (a branch of the maxillary artery), and the infraorbital vein, which connects the inferior ophthalmic vein to the facial vein. The foramen is usually well seen on standard PA (OM = −35°) (Fig. 3) and Waters radiographs (Fig. 4) as well as on tomographic sections (Fig. 7*b*). The floor itself is best evaluated on PA: OM = −35° projection (Fig. 4) to insure that the roof of the sinus is parallel to the beam. AP (Fig. 7*a*, *b*, *c*), and lateral tomograms (Fig. 10*c*) are helpful.

The Inferior Internal Angle (Fig. 11). As noted under the heading "The Medial Wall of the Orbit," above, one may find the lacrimomaxillary suture and groove (with its hamulus lacrimalis) and the ethmoidomaxillary and sphenopalatine sutures here.

The Lateral Wall of the Orbit

The lateral wall is surely the strongest of the four orbital walls. When one approaches the orbital contents laterally during surgery, this buttress must be sawed open. The wall is composed of the greater wing of the sphenoid, the orbital

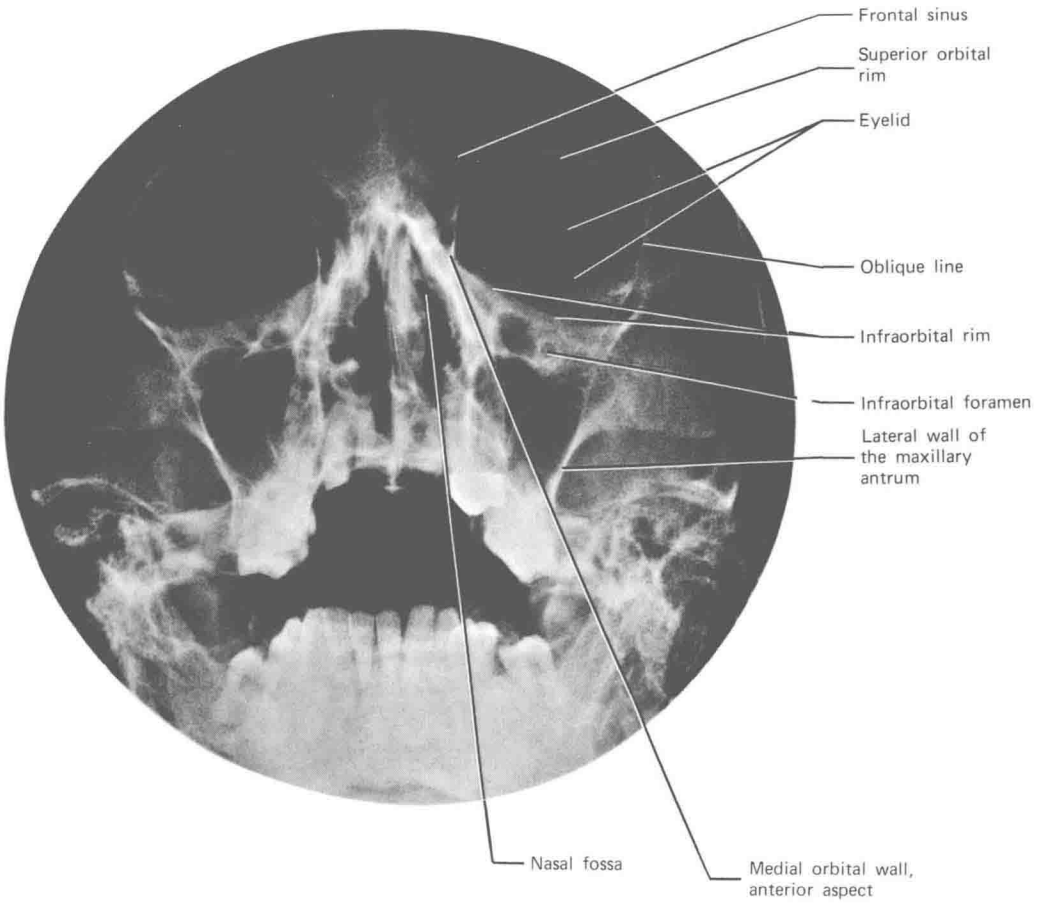

Fig. 4. PA view. OM = −50°.

process of the frontal bone, and the orbital process of the zygoma (Figs. 11, 13).

On the basal radiograph (Fig. 9*a*, *b*, *c*) the lateral wall is seen to run posteromedially, intertwined along its course with the posterior wall of the maxillary sinus. The orbital wall, anterior to the greater wing of the sphenoid (which defines the anterior extent of the middle cranial fossa) pursues a straight course (Fig. 9*a*), while that of the sinus is quite curvilinear (Figs. 5, 9*d*). The optic canal lies just medial to the most posterior extent of the lateral orbital wall. These relations are best seen in basal tomography (Fig. 9*a*).

A small canal (Hyrtl's canal) may be found high on the more posterior aspect of the lateral wall. This canal transmits a small arterial branch from the middle meningeal artery, which supplies the lacrimal gland. Its existence, however, is not constant. The pattern of branching of the embryonic middle meningeal artery is the critical factor in this regard (Fig. 16*a*, *b*).

There is one other structure related to the lateral orbital wall that must be mentioned. The oblique line of the orbit or innominate line (Figs. 2, 3, 7*d*, 8*c*) is not a true anatomic structure. It is an image that is created when the X-ray beam is tangential to the junction of the anterior and lateral aspects of the greater wing of the sphenoid. Distortion or absence of this line may be caused by the presence of orbital or middle fossa pathology.

The Inferior External Angle (Fig. 11). Anteriorly, the angle is formed by the orbital process of the zygoma; posteriorly, it is actually the infraorbital fissure (bound by the greater wing of the sphenoid above and the orbital process of the maxillary below) (Figs. 8*c*, 13).

During life, the orbital periosteum virtually closes the fissure, although it is penetrated by veins joining the orbital veins to the pterygoid plexus. The maxillary nerve (V2) crosses over the fissure on its way to exit from the orbit through the infraorbital foramen, as does a parasympathetic branch from the sphenopalatine ganglion (which innervates the lacrimal gland).

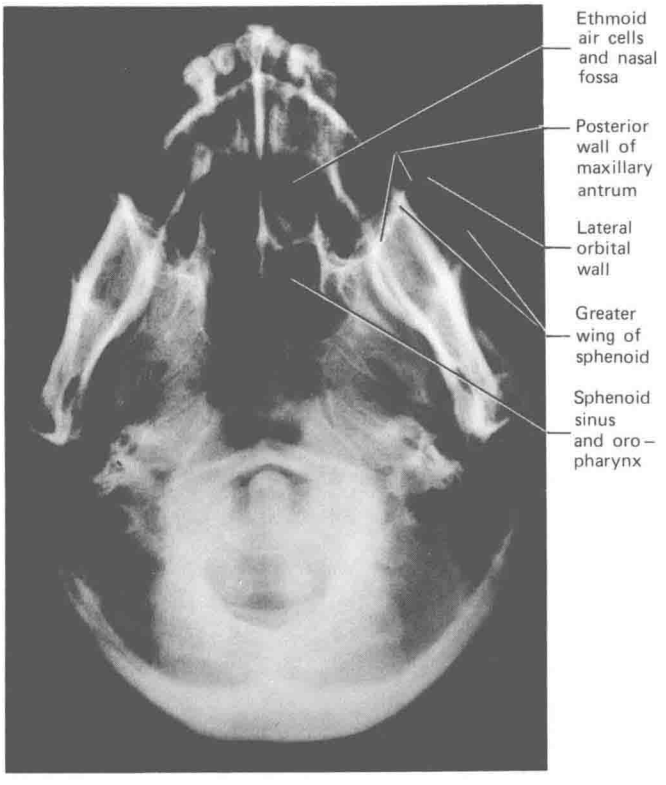

Fig. 5. Basal view. OM = −90°.

The Superior External Angle. The frontosphenoidal suture defines this angle anteriorly, and the superior orbital fissure does so posteriorly. The lacrimal fossa, making up part of the orbital roof, is related to the sphenofrontal suture.

The Base of the Orbit. One can easily follow the bony margin of the base with one's fingers. The components of this ring of compact bone are (Figs. 11 to 13) the orbital arch of the frontal bone, the orbital surface of the zygoma, and the superior portion of the maxilla. There is a notch in the ring superomedially (Fig. 7*a*). The supraorbital notch transmits the supraorbital artery (a branch of the ophthalmic artery) and the supraorbital nerve (a nerve derived from the ophthalmic V1 nerve). The orbital periosteum inserts along this bony ring. Its attachment here is quite firm as opposed to its poor adherence to the orbital walls it carpets.

The Apex of the Orbit. The orbital apex is the area where the four orbital walls and angles converge. The two orifices of the apex, the optic canal and the superior orbital fissure, are situated in the sphenoid bone where the body and greater and lesser wings approximate each other (Figs. 11 to 13).

The optic canal. The optic canal contains the optic nerve and the ophthalmic artery below. Although in the newborn child the canal is only 2 to 3 mm in length, it rapidly elongates during the first few months of life. In the adult, it varies from 6 to 11 mm in length. The axis of the canal is oblique, forming a 35 to 40° angle with the sagittal plane of the skull. It is also angled inferiorly (−35° with relation to the OM line).

At its orbital end (Figs. 11 to 17), the canal is 6 mm in height and 5 mm in width (the greatest diameter varies from 3 to 6.5 mm; Goalwin, 1927; Evans, 1943). The canals are symmetric, varying 1 mm or less in 98% of normal skulls (Goalwin, 1927). In making measurements of the canal, one must remember that the ophthalmic artery runs inferolaterally to the nerve. In cases where the floor of the cranial end of the canal is absent (4% of the population; Kier, 1966) the ophthalmic artery may groove the bone (Fig. 18). Its appearance is quite characteristic ("keyhole anomaly"). Occasionally, the artery may appear to have its own canal. Instead of being a true dual optic canal, this variant exists because of a duplicate cranial opening (1.2% of the population; Kier, 1966). Below and slightly lateral to the orbital aspect of the canal is the infraoptic tubercle. This bony eminence provides a point of attachment of the tendon of Zinn.

The cranial aspect of the canal is bounded by the lesser sphenoid wing and the body of the sphenoid, being located just medial to the root of the anterior clinoid process. Laterally, the canal is separated from the superior orbital fissure by a bony strut. Above, the lesser wing is slightly elongated at the attachment of the dura (falciform reflection) (Fig. 19).

The medial position and angle of emergence of the normal canal preclude visualization on standard AP radiographs. Instead, the head of the patient must be turned 35 to 40° to the side opposite that being examined (Hartmann's projection) (Fig. 17). The beam is angled cranial slightly (−35°). When the canal is projected into the inferolateral quadrant of the orbit, one may be assured that the canal's axis is perpendicular to the film and that positioning is correct. Tomograms in this projection (Fig. 20) may yield information regarding the canal at various depths and the integrity of its margin. One must be quite cautious in looking at the "optic canal." Occasionally a pneumatized anterior clinoid process may appear quite round and may be mistaken for the canal itself (Fig. 21*a*, *b*). By following the planum sphenoidale laterally, one will encounter the true canal. The anterior clinoid process will be just lateral. Tomography in the basal view demonstrates both optic canals on the same view (Fig. 9*a*).

The superior orbital fissure. The superior orbital fissure is the inferomedially directed, club-shaped dehiscence between the lesser sphenoid wing above and the greater wing below (Figs. 11, 13, 22).

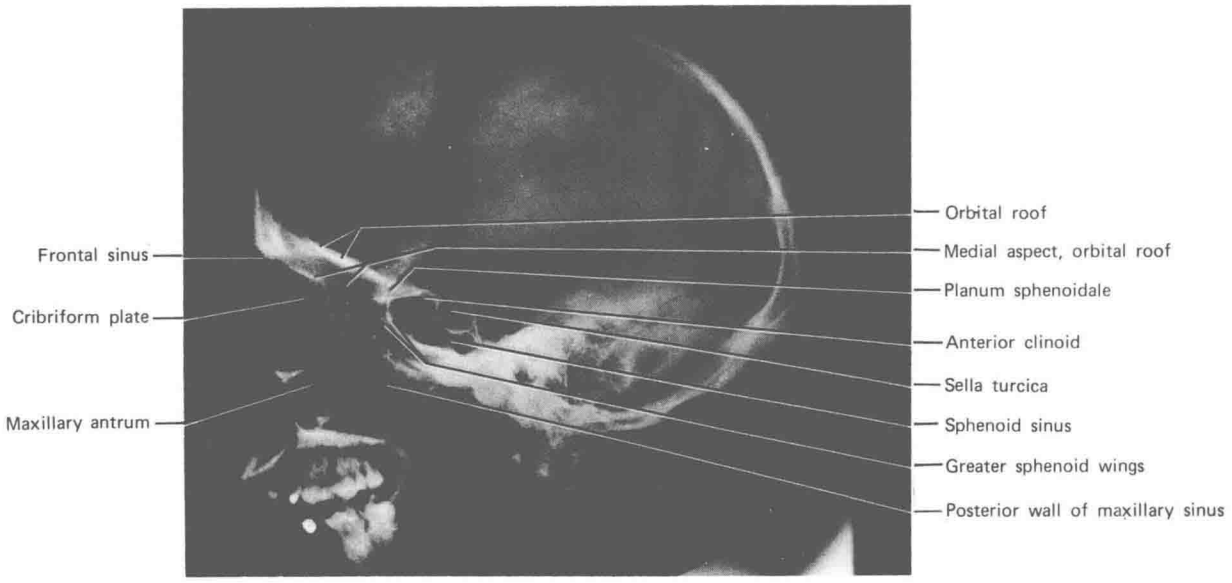

Fig. 6. Lateral view.

Normally the two fissures are asymmetric, and one must exercise caution in ascribing pathologic significance to mere asymmetry without further corroborative findings (e.g., erosion of the cortical margin). Much of the superolateral portion of the fissure is closed by the orbital periosteum, while the entrance of the neurovascular elements into the orbit is found inferomedially. One may group these elements as to whether or not they traverse the tendon of Zinn. In the first group, those outside the tendon, one finds (Fig. 23):

1. The recurrent meningeal artery, uniting the middle meningeal to the lacrimal artery.
2. The lacrimal nerve (a branch of V_1), which receives a parasympathetic branch from the sphenopalatine ganglion.
3. The frontal nerve (a branch of V_1).
4. The trochlear nerve (IV).
5. The superior ophthalmic vein.
6. The inferior ophthalmic vein.

Traversing the annulus of Zinn (from top to bottom) are:

1. The superior branch of the oculomotor (III) nerve.
2. The basal nerve (a branch of V_1).
3. The sympathetic root of the ciliary ganglion.
4. The inferior branch of the oculomotor (III) nerve.
5. The middle ophthalmic vein, if present.
6. The abducens nerve (VI).

THE OCULAR MUSCLES (FIG. 24a,b)

Six striated (skeletal) muscles hold the eyeball in place and are responsible for its movement. All six are of mesodermal origin. They are:

1. The recti.
   a. Superior rectus.
   b. Inferior rectus.
   c. Medial rectus.
   d. Lateral rectus.
2. The obliques.
   a. Superior oblique.
   b. Inferior oblique.

Five of the six muscles originate at the orbital apex. The inferior oblique attaches to the medial aspect of the orbital rim. They are all enclosed within a fibrous capsule known as the capsule of Tenon. The muscles and their fibrous envelope constitute the musculoaponeurotic cone of the orbit, which inserts on the globe. The optic nerve runs through this cone (Figs. 23 to 27).

The levator palpebrae superioris, although not actually one of the ocular muscles, also takes its origin from the orbital apex. It, however, inserts on the upper eyelid.

The four recti originate from the tendon of Zinn, a fibrotendinous band that inserts on the medial portion of the superior orbital fissure and on the infraoptic tubercle (see above). The tendon is 2 mm in width and 5 to 6 mm in length. Its superolateral band divides *proximally* to create